Modeling fire-driven deforestation potential in Amazonia under current and projected climate conditions

Le Page, Y.; van der Werf, G.R.; Morton, D.C.; Pereira, J.M.C.

published in
Journal of Geophysical Research
2010

DOI (link to publisher)
10.1029/2009JG001190

document version
Publisher's PDF, also known as Version of record

Modeling fire-driven deforestation potential in Amazonia under current and projected climate conditions

Y. Le Page,[1] G. R. van der Werf,[2] D. C. Morton,[3] and J. M. C. Pereira[1]

Received 27 October 2009; revised 1 March 2010; accepted 15 April 2010; published 7 August 2010.

[1] Fire is a widely used tool to prepare deforested areas for agricultural use in Amazonia. Deforestation is currently concentrated in seasonal forest types along the 'arc of deforestation', where dry-season conditions facilitate burning of clear-felled vegetation. Interior Amazon forests, however, are less suitable for fire-driven deforestation due to more humid climate conditions. These forests will ultimately come under more intense pressure as the deforestation frontier advances. Whether these regions continue to be protected by humid conditions partly determines land use changes in interior Amazon forests. Here, we present a study of the climate constraint on deforestation fires in Amazonia under present-day and projected climate conditions. We used precipitation data and satellite-based active fire detections to model fire-driven deforestation potential. Our model results suggest that 58% of the Amazon forest is too wet to permit fire-driven deforestation under current average climate conditions. Under the IPCC B1 scenario, the model indicates increased fire potential by 2050 in eastern Amazonia, while dry-season precipitation may provide limitations on projected deforestation by 2050 in central and western Amazonia. However, the entire region is very sensitive to a possible drying with climate change; a reduction in dry-season precipitation of 200 mm/year would reduce the climate constraint on deforestation fires from 58% to only 24% of the forest. Our results suggest that dry-season climate conditions will continue to shape land use decisions in Amazonia through mid-century, and should therefore be included in deforestation projections for the region.

Citation: Le Page, Y., G. R. van der Werf, D. C. Morton, and J. M. C. Pereira (2010), Modeling fire-driven deforestation potential in Amazonia under current and projected climate conditions, *J. Geophys. Res.*, *115*, G03012, doi:10.1029/2009JG001190.

1. Introduction

[2] Global demands for food crops, animal ration, and agricultural biofuels have intensified efforts to expand worldwide agricultural production [*Naylor et al.*, 2005]. The search for new crop and pasturelands contributes to tropical deforestation [*Morton et al.*, 2006], as large areas of tropical forest are suitable for agriculture use [*Balmford et al.*, 2005; *Nepstad et al.*, 2008]. The Brazilian Amazon accounted for nearly half of all tropical deforestation during 2000–2005 [*Hansen et al.*, 2008], where cumulative forest losses for agricultural expansion over the last 20 years cover an area equivalent to the size of Spain (Brazilian National Institute for Space Research (INPE), PRODES project, available at http://www.obt.inpe.br/prodes/).

[3] Fire is the dominant method to remove forest biomass during the deforestation process. In Amazonia, the clearing sequence begins with clear-felling trees during the wet season, and deforested areas are then allowed to cure before burning occurs during dry-season months [*Carvalho et al.*, 2001]. Along the existing 'arc of deforestation', three to five months with little rainfall may permit multiple fires in the same dry-season. After the first fire, unburned trunks, branches and roots can be mechanically piled and burned repeatedly [*Morton et al.*, 2008]. From a climate change perspective, repeated burning results in rapid loss of the majority of carbon in aboveground biomass to the atmosphere, with little compensation by regrowing vegetation in crops or pastures [*Morton et al.*, 2008; *van der Werf et al.*, 2008a]. Current forest conversion pressure is highest in regions where the dry-season is long enough to permit fire-driven deforestation. However, the deforestation frontier is advancing into less seasonal forest types, where more humid conditions limit fire efficiency [*van der Werf et al.*, 2008b]. Currently, there is no cost-effective alternative to fire for clearing large areas of tropical forests.

[4] Future degradation of the Amazon forest will thus partly depend on the climatic conditions that govern fire

[1]Departamento de Engenharia Florestal, Instituto Superior de Agronomia, Lisbon, Portugal.
[2]Department of Hydrology and Geo-environmental Sciences, Faculty of Earth and Life Sciences, VU University Amsterdam, Amsterdam, Netherlands.
[3]NASA Goddard Space Flight Center, Greenbelt, Maryland, USA.

0148-0227/10/2009JG001190

deforestation potential (FDP) and on a confluence of other factors: (1) The definition and application of conservation policies, i.e., protected areas [*Nepstad et al.*, 2006], or preservation incentives [*Ebeling and Yasue*, 2008; *Hall*, 2008]; (2) the dynamics of agricultural expansion and logging pressure [*Morton et al.*, 2006; *Soares-Filho et al.*, 2006]; (3) the eco-climatic requirements for agricultural use [*Jasinski et al.*, 2005; *Nepstad et al.*, 2008]; (4) the development of new transport infrastructure [*Nepstad et al.*, 2001]; (5) the resilience of the forest to changes in climate conditions [*Mayle and Power*, 2008; *Mayle et al.*, 2007] and to anthropogenic disturbances such as fire [*Cochrane and Laurance*, 2008].

[5] Recent modeling efforts to predict deforestation dynamics in the coming decades integrate many of these key factors [*Michalski et al.*, 2008; *Soares-Filho et al.*, 2006]. Deforestation projections provide insights into the suitability of forested land for agricultural use on the basis of infrastructure availability, conservation policies, and socio-economic factors. However, they do not consider whether climate conditions will permit fire-driven deforestation. On the other hand, fire modeling aproaches account for the role of climate [*Arora and Boer*, 2005; *Cardoso et al.*, 2003, 2008; *Golding and Betts*, 2008; *Thonicke et al.*, 2001], but deforestation practices which alter fire susceptibility and fire incidence are not represented (i.e., clear-fells, vegetation piling, multiple ignitions). These models thus give little information about the spatial feasibility of large-scale tropical forest conversion. Two recent studies identified the dependence of deforestation on fire efficiency, and thus on climate, based on monthly or seasonal drought indices [*Aragao et al.*, 2008; *van der Werf et al.*, 2008a].

[6] Here we built on these studies and developed a model of fire-driven deforestation potential (FDP) based on precipitation data and satellite-based deforestation fire detections to define the current climatic envelope for large-scale deforestation in the Amazon. We propose a methodology addressing the issue at a 10-day time scale consistent with vegetation and soil moisture dynamics and the anthropogenic readiness to take advantage of short dry windows to ignite fires [*Uhl and Kauffman*, 1990]. We then ran the model using current (1980–2000) precipitation data and projections of 2050 climate to (1) study how climate change may impact the area of Amazon forest in which fire-driven deforestation is possible, and (2) evaluate the fraction of projected forest loss by 2050 that falls within regions with high FDP. Finally, we considered how annual or seasonal decreases in precipitation alter FDP, to quantify the resulting retreat of the climatic constraint for human-dominated landscapes in Amazonia.

2. Data and Methods

2.1. Data

2.1.1. Deforestation Fires

[7] The deforestation fire data set from [*Morton et al.*, 2008] is based on a subset of the MODIS collection 4 fire detections product [*Justice et al.*, 2002], taking only the high-confidence fire detections into account to eliminate the false alarms detected frequently at the forest-agriculture interface [*Schroeder et al.*, 2008]. The methodology to separate deforestation fires from other types of fires is based on the practice of repeated fires at the same location in preparation for agricultural use; detections of two or more fires during the same fire year within a 1 km radius are tagged as deforestation fires. A fire year is defined as July–June north of the equator, January–December in the southern hemisphere. Two non-deforestation fires on separate days within a 1 km radius could be mistakenly flagged as deforestation fires. *Morton et al.* [2008], however, suggested that most non-deforestation fires were excluded from the data set (10% commission error in the Brazilian state of Mato Grosso in southern Amazonia). The impact of potential commission errors on model parameterization is further minimized by the consistent seasonality of deforestation and other fire types in Amazonia. We selected data from both Terra and Aqua satellites to maximize the sampling of the daily fire cycle, resulting in 4 complete fire years (mid 2002–2006). Daily 1 km deforestation fire detections were aggregated to 1° × 1° spatial resolution for three ~10-day intervals each month, calculated as two 10-day periods from the 1st to 20th, and one 8- to 11-day period from the 21st to the end of the month.

2.1.2. Climate Observations

[8] Daily precipitation rates at 1° × 1° resolution over 2002–2006 were obtained from the Global Precipitation Climatology Project (GPCP) version 2, which combines various data sources [*Huffman et al.*, 2001]. At this resolution, some relevant spatial variability in precipitation patterns may not be accounted for in the model parameterization. However, previous studies suggest large errors in fine-scale precipitation products available over the 2002–2006 model development period, which can be minimized by spatiotemporal aggregation as applied here [*Huffman et al.*, 2007]. Over 1979–1999, we used the pentad (5-day) precipitation data set at 2.5° × 2.5° resolution from the CPC merged Analyses of Precipitation (CMAP [*Xie and Arkin*, 1997]), provided by the NOAA/OAR/ESRL PSD, Boulder, Colorado, USA, (http://www.cdc.noaa.gov/). Both data sets were aggregated to 10-day periods and the CMAP data was regridded to 1° × 1° to match the resolution of the deforestation fire data.

2.2. Model Development

[9] Deforestation fires are the culmination of numerous factors that drive land use decisions in Amazonia (Figure 1). Here, we focused on the climate-mediated potential for fire-driven deforestation. Figure 2 shows 10-day time series of deforestation fires and precipitation over 2003–2006 for three grid-cells. Precipitation patterns define the seasonal timing of fire activity; fires only occur during the dry-season, mostly as late season fires [*Schroeder et al.*, 2005]. At an intraseasonal time scale, wet 10-day periods within the dry-season result in a drop of deforestation fire activity (e.g., last 10-day of August 2004 in Mato Grosso). These examples suggest that climate can dissuade human ignitions and/or influence whether these fires will be successful through direct impacts on vegetation and soil moisture (Figure 1, arrows a, b, d, f, and h). Finally, fire activity also varies significantly at inter-annual time scale: Figure 2a illustrates how drought conditions in Rondônia in 2005 increased deforestation fire potential.

[10] Since we aim to model the potential use of fires, independent of any deforestation projections, climate is the factor to isolate. However, factors of anthropogenic origin

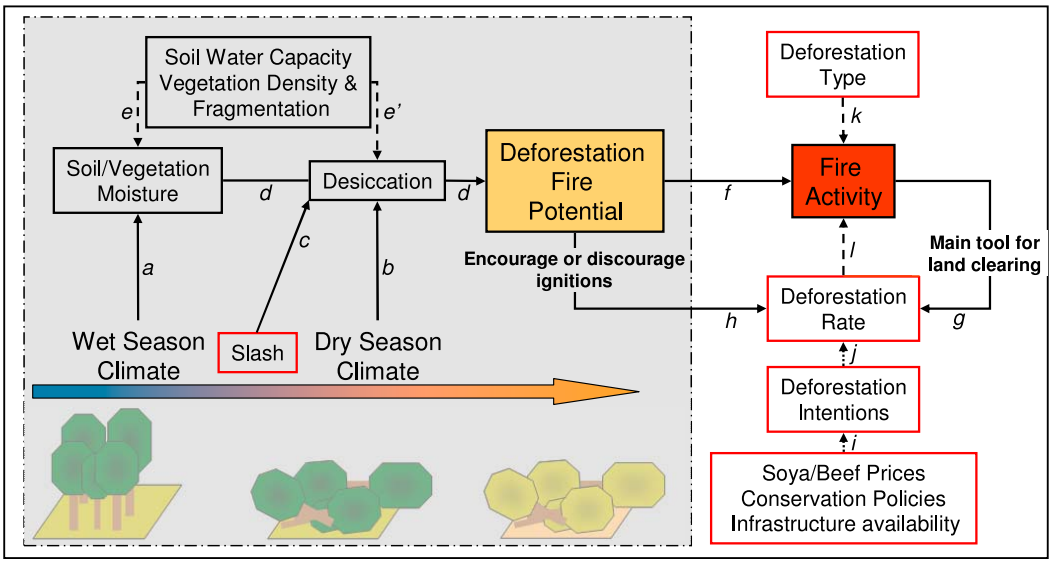

Figure 1. Interactions among climate, vegetation and anthropogenic factors in the context of fire-driven deforestation. Climatic conditions govern fuel moisture following deforestation, described as the deforestation fire potential, whereas land-use decisions on the amount and type of agricultural expansion in Amazon regions ultimately determine the fire activity within periods with suitable climate for fire-driven deforestation. Feedbacks from deforestation on local climate or moisture dynamics due to fragmentation were excluded.

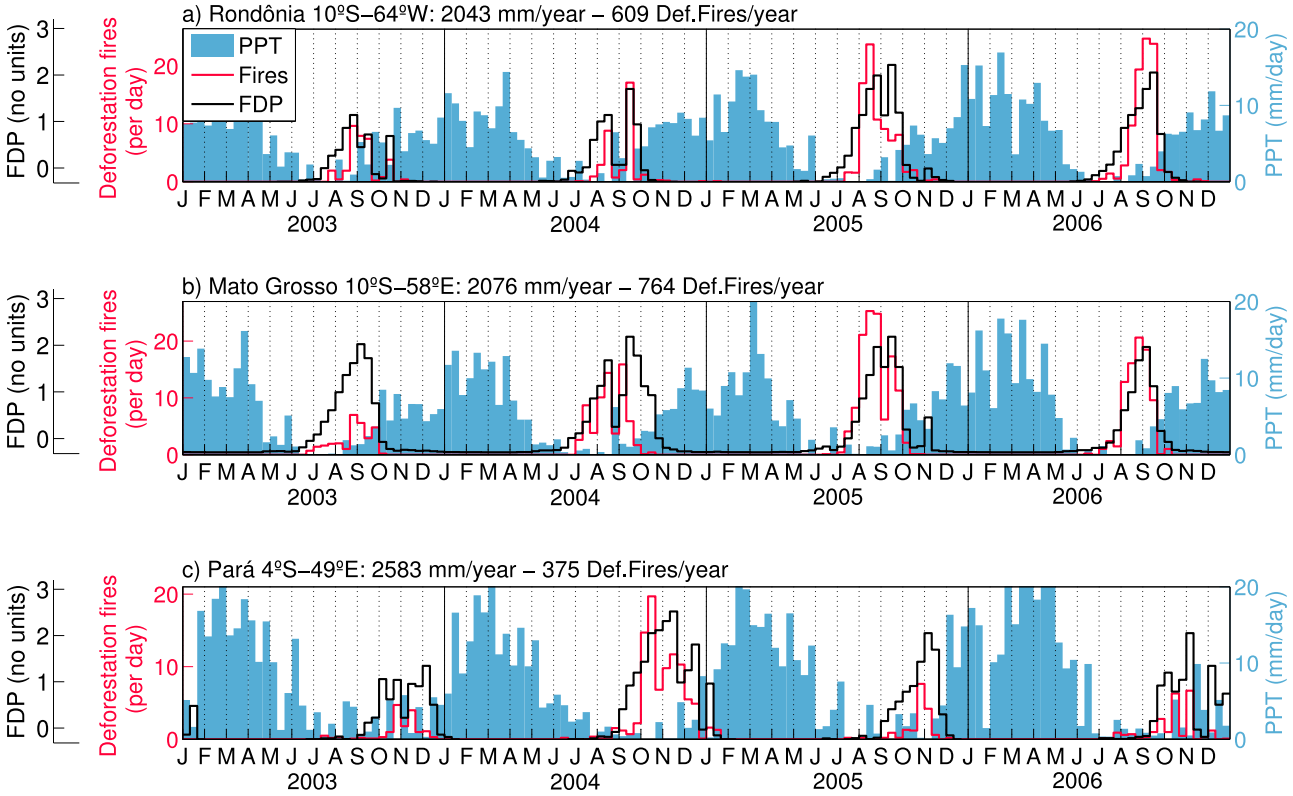

Figure 2. Ten-day time series of precipitation rates (blue bars), deforestation fire detections (red stairs), and Fire Deforestation Potential (FDP, black stairs), during 2003–2006 for three 1° × 1° cells in southern Amazonia.

are also involved, and need to be taken into account to characerize climate-driven variability. First, vegetation curing is intentionally accelerated by cutting trees, preventing them from accessing groundwater (Figure 1, arrow c). Second, humans decide whether or not to burn during a fire prone climatic window. In Rondônia for example, increased fire activity in 2005 (845 deforestation fires versus 354 in 2004) may have various explanations. Economic incentives for deforestation may have been stronger in 2005 (arrows i and j), possibly aided by new infrastructure facilitating deforestation (arrows i and j). Alternatively, 2004 had a rather moist dry-season which may have limited the use of fires (through arrows a and b, and see Figure 2a), while drought conditions prevailed in 2005 [*Marengo et al.*, 2008]. The predominant type of deforestation could also be involved (arrow k); in the state of Mato Grosso conversion to cropland involves nearly three times as many fires as conversion to cattle ranching [*Morton et al.*, 2008]. Unfortunately, information about these anthropogenic factors is not always available at the spatiotemporal resolution required to perform satisfying statistical analyses at the scale of the Amazon. One could argue that gridded information on deforestation rates [*Achard et al.*, 2007; *Hansen et al.*, 2008] provide a single proxy accounting for the combined influence of these factors, and could be used to remove the fire variability due to changes in deforestation pressure rather than climate variability. A drawback of this approach is that deforestation and fires are both a cause and a consequence of each other: a lower deforestation rate may be either the cause of decreased fire activity (arrow l, unwanted variability) or its consequence if climate was too humid (arrows f, g, and h, variability under study).

[11] Consequently, building a fire-potential model required transforming the fire observation data to make it independent on the extent and type of deforestation. This was partially achieved by computing intra-annual fire anomalies for each grid-cell and each year, based on two assumptions:

[12] 1. The anthropogenic will to deforest is rather constant within a year, i.e., conversion plans are decided early and do not change much over the course of the dry-season (other than for climatic reasons), and economic or political factors impacting deforestation are stable at an annual time scale.

[13] 2. The distribution of deforestation fires within a year is mostly driven by climate, other potential drivers being considered insignificant. [*Morton et al.*, 2008], for example, showed that the intra-annual timing of fires changes slightly with conversion type.

[14] Fire intra-annual anomalies were computed as:

$$Fa_{y,d} = \frac{F_{y,d} - mean\left(F_{y,d=1:36}\right)}{std\left(F_{y,d=1:36}\right)}$$

where $F_{y,d}$ is the fire activity during the 10-day period d of year y (36 10-day periods per year), and $Fa_{y,d}$ the corresponding fire anomaly. To avoid unrealistic anomalies, we discarded 1° × 1° grid-cells with a peak fire activity of less than 10 fires in a 10-day period, and years with less than four 10-day periods with observed fires.

[15] To study the relationship between fire anomalies and climate, we defined two indicators of moisture conditions based on Figure 1, detailed observations of the data (as in Figure 2), and reported deforestation practices:

[16] 1. The long-term precipitation (LTppt) variable represents the vegetation sensitivity to fires due to climate conditions on monthly timescales. This indicator captures desiccation dynamics of the slashed trees (fuels) during the dry-season, as fire efficiency increases with curing time following clear-felling of vegetation [*Carvalho et al.*, 2001]. LTppt is calculated as follows:

$$LTppt_d = \frac{\sum_{\mathrm{i=d-m}}^{\mathrm{d-1}} \mathrm{PPT_i} \times (b + i - (d - m))}{(\mathrm{b} + 1) \times m}$$

where d is the current 10-day period, m the number of previous 10-day periods to be considered (the "memory" of the indicator), PPT_i the precipitation at 10-day period i, and b a constant value controlling the decrease of the weight of 10-day periods with time (conditions during the most recent 10-day periods have a greater impact on LTppt). Various studies point at a delay of two to five months after the wet season to reach significant fire sensitivity [*Carvalho et al.*, 2001; *Field and Shen*, 2008; *Schroeder et al.*, 2005; *van der Werf et al.*, 2008a]. Accordingly, we apply a memory (m) of 15 10-day periods, equivalent to 5 months. We tested a range of value for the parameter b, which we set to $b = 6$ by visual inspection, meaning that precipitation during the most recent 10-day period is three times as important as the oldest (15th) 10-day period in computing LTppt. Note also that LTppt does not depend on precipitation during the 10-day period under consideration, which is captured with the short-term precipitation parameter (see below).

[17] 2. The short-term precipitation (STppt) variable, which represents the vegetation sensitivity to fires due to climate conditions over recent days. The STppt metric captures the rapid dynamics of superficial moisture due to daily weather [*Holdsworth and Uhl*, 1997; *Ray et al.*, 2005; *Uhl and Kauffman*, 1990]. This indicator is taken as the weighted mean of the precipitation over the considered (weighting 75%) and previous (weighting 25%) 10-day period.

[18] For each grid cell and for each 10-day period we computed fire anomalies, LTppt and STppt. LTppt and STppt were binned into 25 equal intervals, and each fire anomaly was attributed to the observed LTppt and STppt. To strengthen the independence of the results to other sources of variability that may limit fire use even under favorable climate conditions, the fire deforestation potential (FDP) under each LTppt/STppt pair was then computed as the upper quartile (at 0.75) of the corresponding fire anomalies (Figure 3, left). These results were finally smoothed to avoid unrealistic behavior of the final model (using a classic moving window average filter and forcing a decreasing FDP along increasing LTppt and STppt), as presented in Figure 3 (right). A second metric, the annual fire deforestation potential (anFDP), is defined as the sum of all positive 10-day FDP values in a given year (negative values of FDP always result in no or insignificant fire activity). Fire anomalies as used here represent the fire climate potential, i.e., under what climatic conditions do the fires actually burn in a given year. Although raw anomalies are not quantitative, the removal of unrealistic anomalies,

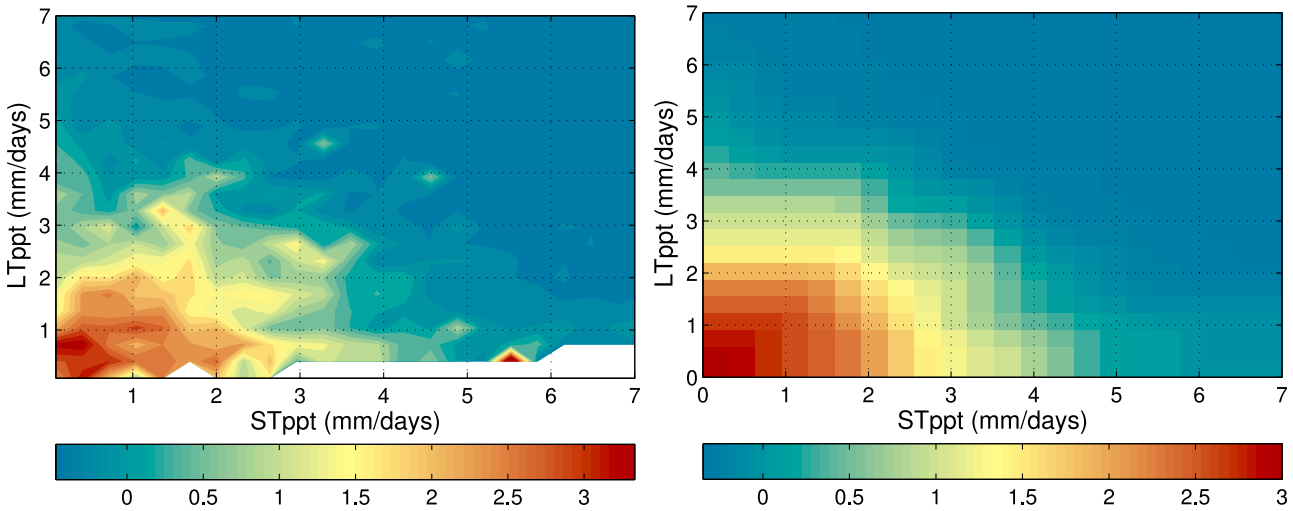

Figure 3. (left) Contour plot of the upper-quartile FDP based on climate and fire detections during 2002–2006 and (right) final model configuration after smoothing. FDP is unitless (standardized anomalies).

the use of the upper quartile, and the annual aggregation make of the anFDP metric a relevant indicator of the maximum fire activity possible during a given dry season (see section 3).

[19] We excluded several factors in our model that influence moisture dynamics (Figure 1, arrows e and e'), including forest fragmentation [*Broadbent et al.*, 2008; *Laurance and Williamson*, 2001], vegetation type and density [*Saatchi et al.*, 2007] and soil water retention capacity [*Nepstad et al.*, 2004]. Further, our model represents moisture conditions with two indicators based on precipitation, while temperature also modulates evapotranspiration rates. We chose not to include temperature in the model as it shows little seasonality in most tropical forests, indicating that moisture anomalies are largely a function of precipitation.

2.3. Climate and Deforestation Scenarios

2.3.1. Deforestation Scenarios

[20] To estimate how climatic conditions may impact deforestation in the coming decades, we used deforestation projections developed by *Soares-Filho et al.* [2006]. Their model runs at 1km resolution with annual time steps, based on recent deforestation trends, infrastructure availability (proximity to roads, towns and rivers), biophysical features (e.g., soils, slope) and protected areas, with distinct simulation parameters for each of the 47 socio-economic subregions defined in the Amazon basin.

2.3.2. IPCC Climate Scenarios

[21] Precipitation projections were computed from the Intergovernmental Panel on Climate Change (IPCC) AR4 General Circulation Model (GCM) runs [*IPCC*, 2007], provided by the World Climate Research Programme's (WCRP's) Coupled Model Intercomparison Project phase 3 (CMIP3) multimodel data set. We selected the A2 and B1 greenhouse gases emission scenarios to provide high and low estimates of projected climate changes, respectively. A2 represents a differentiated world, with slow transfers of new technologies, and the highest population trajectory. B1 represents a convergent world, with the development of clean and efficient technologies and a lower population trajectory.

[22] Precipitation projections have been made available by the IPCC, using the Climate Research Unit (CRU) Global Climate Data set [*Mitchell and Jones*, 2005] as the climatological baseline to which is applied the projected change of a given scenario compared to the reference scenario (called 20C3M, forced with greenhouse gas concentration changes observed through the 20th century). A preliminary assessment of the CRU precipitation data over the Amazon revealed important discrepancies, up to 1500 mm/year in some regions. Given the sensitivity of fires to small changes in climate conditions, this bias was not acceptable for our study. We thus retained the CMAP data, with a much better agreement, as our climatological baseline over 1979–1999.

[23] We computed projections from all IPCC models for which both the A2 and B1 scenarios were available (17 models), over the 2049–2069 period (year 2049 for LTppt computation in 2050). Due to limitations in computing capacities we used monthly rather than daily model outputs to compute the precipitation change ratio. The same ratio was thus applied to each monthly group of three 10-day periods of the climatological baseline, which downsamples the eventual annual cycle in climatic anomalies, but not the variability at the 10-day time scale which is conserved from the baseline data. There was little agreement within the 17 IPCC models used, with some models projecting much drier conditions over a large area of the Amazon, and others suggesting little change or increased precipitation. Averaged over all models, precipitation did not change much over most grid-cells. We therefore show the lower (0.25) and upper (0.75) quartile of the projected FDP to represent the inter-model variability.

2.3.3. Statistical Climate Scenarios

[24] As an alternative to climate model projections, we estimated the precipitation reductions necessary to reach three thresholds of annual deforestation fire potential (low, high, and unlimited, as defined in section 3.1). We gradually altered the CMAP 1979–1999 precipitation data toward drier

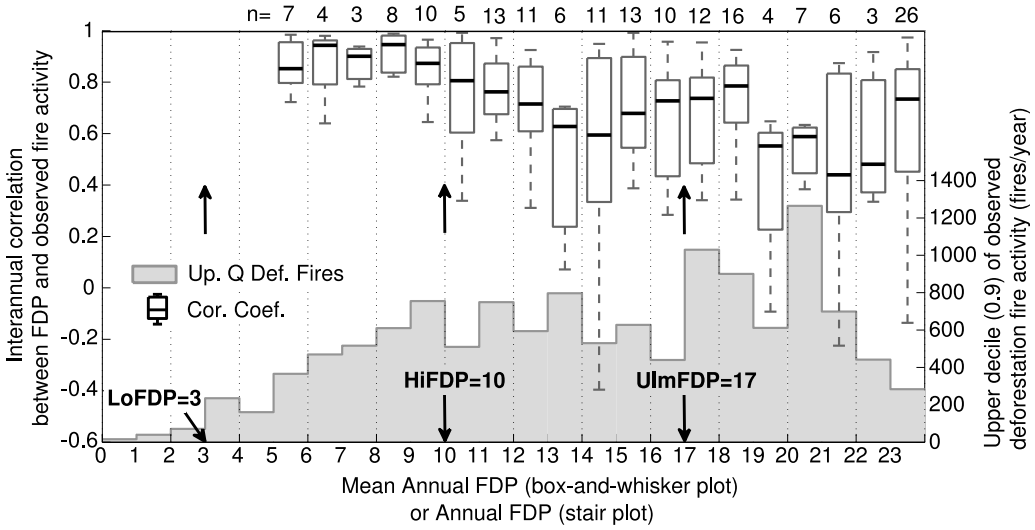

Figure 4. Climate constraint on deforestation fires in the Amazon over 2002–2006. Box-and-whisker plots: for each grid-cell within the corresponding mean anFDP interval (]0 1],]1 2], etc.), the correlation between the time series of anFDP and observed deforestation fires (4 years) is computed. The box represents the median, upper and lower-quartile values of the correlation coefficients. The whiskers represent the most extreme values within 1.5 times the inter-quartile range from the end of the box (standard). The number of grid-cells to build each box-and-whisker is indicated on top. The stair plot represents the 0.9 upper-decile of the observed deforestation fire activity as a function of anFDP. anFDP = 3 (LoFDP), anFDP = 10 (HiFDP) and anFDP = 17 (UlmFDP) are the low, high and unlimited anFDP thresholds defined on the base of these results (see text).

conditions and ran the FDP model at each step, following two different methodologies. In the first case, the annual decrease in precipitation was evenly distributed over all 10-day periods with nonzero precipitation to simulate a "uniform" climate change scenario. In the second case, decreases in preciptation were attributed to the 10-day period with least (but nonzero) precipitation, thus concentrating the change over the dry-season, as a simulation of enhanced "seasonal" climate change.

3. Results

3.1. Fire Potential Under Current Conditions

[25] We plotted observed fires and FDP together to provide a qualitative comparison of actual and potential fire activity (Figure 2). Although they are not directlty comparable, since FDP is only dependent on climate, the time series indicates a realistic parameterization. At the seasonal scale, FDP and active fires define a similar fire season length. On a 10-day scale, FDP and fire variability are closely related when climate turns less favorable to fires; low FDP results in low fire activity. When fire potential is increasing or high, fire activity is generally elevated, but variable. This variability in fire use during suitable climate periods suggests that drivers other than climate influence landowner decisions for deforestation, and motivated our use of the upper quartile to represent fire potential (section 2.2).

[26] On inter-annual time scales, the correlation between anFDP and annual deforestation fire activity is strongest in the most humid active deforestation areas of Amazonia (Figure 4). In these regions, inter-annual variability in fire activity is thus strongly driven by climate. In more seasonal forest types, the relationship is weaker and more variable, suggesting that deforestation fire activity is less constrained by climate; although drier years allow for more fires, the main source of variability is more likely of anthropogenic origin (section 2.2).

[27] We defined three anFDP thresholds based on the natural breakpoints in Figure 4. Above HiFDP (anFDP = 10), precipitation patterns have less influence on fire potential (high variability of the fire-climate correlation), and significant levels of fire activity are observed. Below HiFDP, precipitation becomes increasingly constraining, and below LoFDP (anFDP = 3), we estimate that the use of fire for deforestation is virtually impossible. This lower limit for fire activity, however, is difficult to quantify, as the wettest regions of the Amazon basin had little deforestation within our study period. Finally, we set a threshold indicating unlimited fire-driven deforestation potential (UlmFDP, anFDP = 17). It corresponds to regions with a long dry-season, where intense deforestation fire activity with numerous repeated burns have been observed.

[28] Most areas of the Amazon basin experienced one or more years with high anFDP during 1980–1999, but deforestation fire activity during 2003–2006 was concentrated in regions with high average anFDP (Figure 5). The model reveals strong north-south gradients in average deforestation fire potential, from high values in southern Amazonia and Roraima State in northern Brazil to low values in equatorial regions of western Amazonia (Amazonas State, southern Colombia, and eastern Perú, Figure 5a). Under average climatic years, 42% of the remaining forest is climatically suitable for fire-driven deforestation (above HiFDP). The conversion of significant areas of these forests

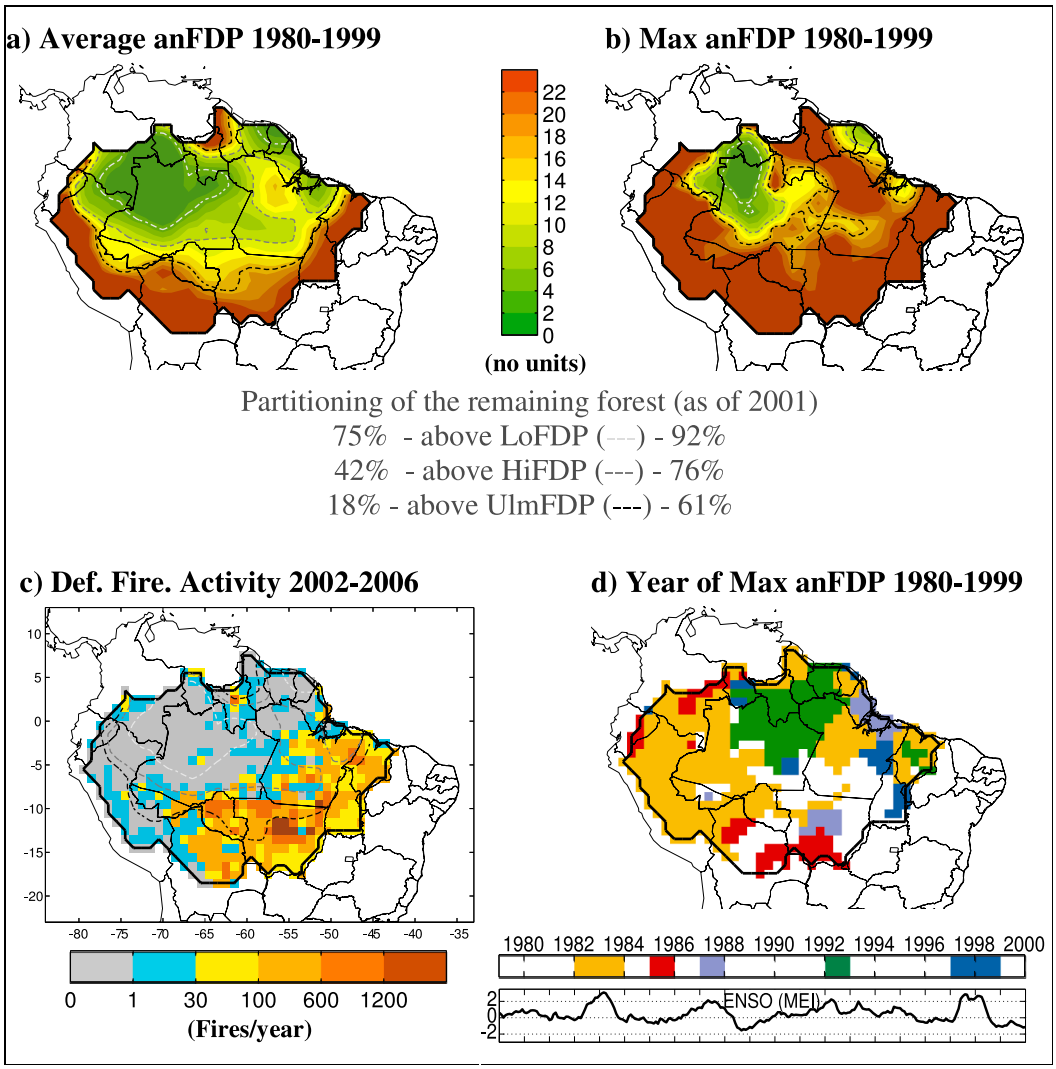

Figure 5. (a) Average and (b) maximum anFDP under 1980–1999 CMAP precipitation conditions. White/gray/black dotted lines indicate the location of the LoFDP, HiFDP and UlmFDP thresholds, respectively. The partitioning of the forest along the three thresholds is based on the remaining forest as of 2001 in the *Soares-Filho et al.* [2006] data. (c) Annual averaged deforestation fire activity over mid 2002–2006. (d) Year of maximum anFDP, along with time series of the MEI ENSO index (from the National Oceanic and Atmospheric Administration (NOAA), http://www.cdc.noaa.gov/people/klaus.wolter/MEI/).

is limited by other factors (e.g., infrastructure, protected areas, and soil suitability), such that deforestation already reached regions with limited fire efficiency for clearing land (below HiFDP), especially in the eastern Amazon basin (Figure 5c). However, the maximum anFDP over these 20 years (Figure 5b) indicates that a large part of the forest under low mean anFDP experienced significant fire potential during drier years, as 76% of the forest exceeded the HiFDP threshold at least one year during 1980–1999. Periods of maximum potential for deforestation fires generally coincide with large-scale drought events, especially with positive anomalies in the El Niño-Southern Oscillation (Figure 5d).

3.2. Fire Potential Under a Changing Climate

3.2.1. IPCC Projections

[29] The projected average deforestation fire potential during 2050–2069 under the B1 and A2 emissions scenarios highlights the large range of climate model projections for the Amazon region (Figures 6a and 6b). Unexpectedly, both scenarios yielded very similar results (Figure 6e), which has not been previsouly reported to our knowledge. We thus focus our discussion on the results from the B1 scenario mostly. In the B1 lower quartile case, the forest area in each anFDP category in 2050 is slightly lower than under current climate conditions (Figure 6e). In the upper quartile case, the HiFDP boundary expands to 63% of remaining forest areas versus 42% under current climate conditions. Changes in AnFDP by 2050 were concentrated in eastern Amazonia, while interior Amazon forests retained low anFDP values in 2050 even in the upper quartile of B1 projections (Figure 6d). As a result, a substantial portion of projected deforestation by 2050 could be limited by precipitation constraints on fire-driven forest clearing (Figures 6c and 6e). Based on average anFDP years, climate conditions could limit 1/3–1/2 of

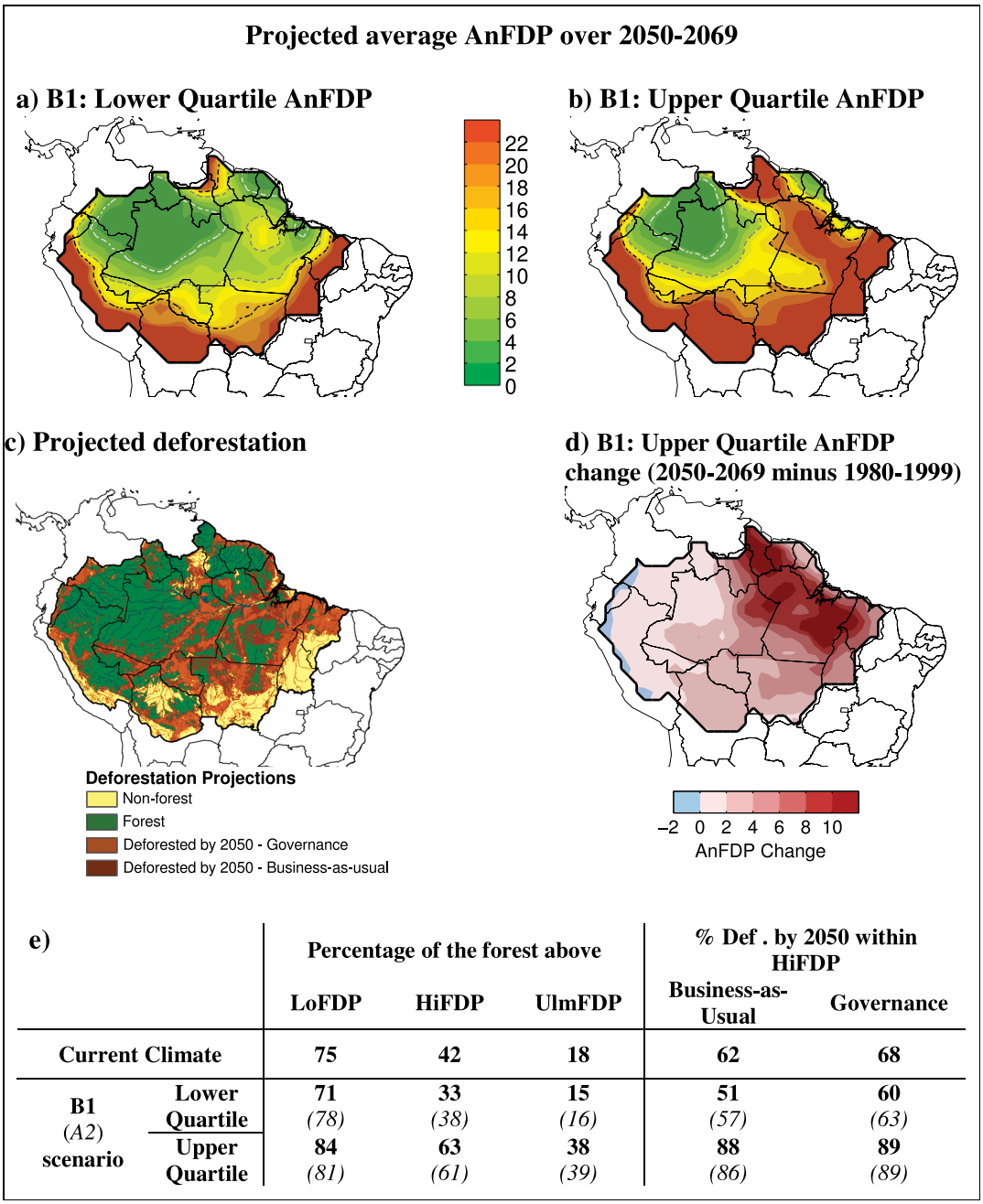

e)

		Percentage of the forest above			% Def . by 2050 within HiFDP	
		LoFDP	HiFDP	UlmFDP	Business-as-Usual	Governance
Current Climate		75	42	18	62	68
B1 (*A2*) scenario	Lower Quartile	71 *(78)*	33 *(38)*	15 *(16)*	51 *(57)*	60 *(63)*
	Upper Quartile	84 *(81)*	63 *(61)*	38 *(39)*	88 *(86)*	89 *(89)*

Figure 6. (a) Lower and (b) upper quartile of the projected average AnFDP over 2050–2069 under the B1 scenario. (c) Projected deforestation by 2050 [*Soares-Filho et al.*, 2006]. (d) Change in AnFDP for the B1 upper quartile run, to highlight regional changes. (e) Partitioning of the Amazon forest (as of 2001) above the three anFDP thresholds, and percentage of the projected deforestation assessed to be feasible with fire by the model.

projected deforestation by 2050 under current climate conditions or the B1 lower quartile case. Results for the upper quartile of B1 projections suggest that only 11–12% of projected deforestation would face climate limitations to fire-driven deforestation during the 2050–2069 period.

3.2.2. How Much Change in Precipitation Will Make the Forest Vulnerable to Fire?

[30] Model runs with the iterative precipitation change (section 2.3.3) reveal a great sensitivity of anFDP to seasonal changes in precipitation, and indicates that a substantial portion of the remaining forest is close to a climatic regime no longer limiting fire-driven deforestation (Figure 7). With a loss of 200 mm of precipitation over the dry-season, the percentage of the forest above HiFDP would increase from 42% to 64% and 76% in the uniform and seasonal change case, respectively. Considering the UlmFDP threshold, at which intense deforestation fire activity is currently observed and climate constraints are minimal, the 200mm change

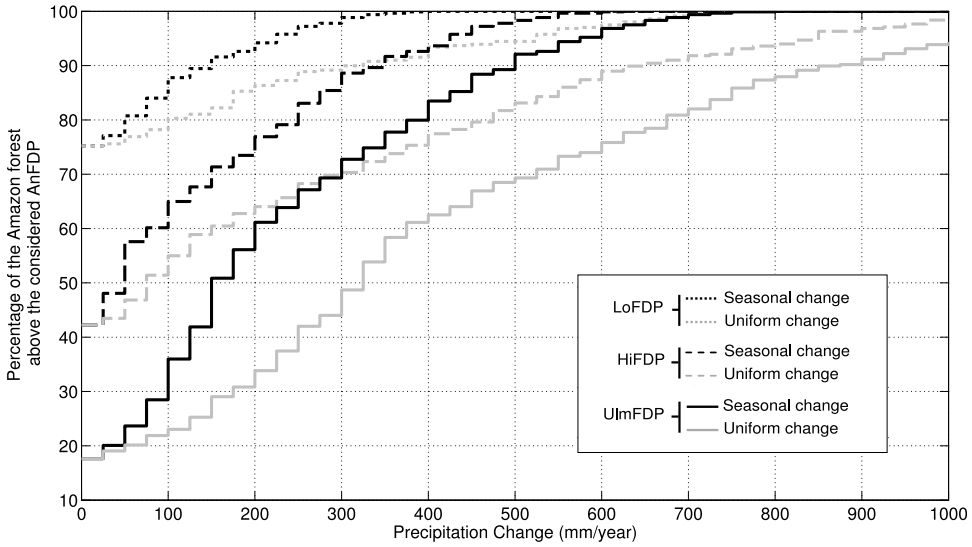

Figure 7. Proportion of the Amazon above the three anFDP thresholds considered (LoFDP, HiFDP and UlmFDP) as a function of two types of precipitation change. Seasonal change is distributed over the driest 10-day periods, while the uniform change scenario distributes reductions in precipitation evenly throughout the year (see text).

results in an increase from 18% to 34% (uniform) and 61% (seasonal). For the seasonal change case, the climatic distance to go from LoFDP to HiFDP amounts to ~200 mm, and to 100–150 mm from HiFDP to UlmFDP.

4. Discussion

4.1. Strong Limitation for Deforestation Progression Under Current Climate

[31] We estimate that more than half (58%) of the remaining forest of the Amazon is currently protected by climate against fire-driven deforestation. In these areas, average dry-season conditions are neither long nor dry enough to reach high fire potential. The location of the existing deforestation frontier now abuts these regions with reduced suitability for fire-driven deforestation. Although large uncertainties remain on the role of climate, global economy, and policies in driving annual deforestation rates, climate is thus likely to be a critical factor as the frontier expands into these regions. AnFDP increases dramatically during drought episodes, rendering fire-driven deforestation possible across much of Amazonia; from 1980 to 1999, only 24% of the forest never reached HiFDP fire prone conditions. These droughts provide opportunities to intensify fire practices and are associated with accidental understory fires, as illustrated in 2005 with a 43% increase in the number of fires per deforested unit [*Aragao et al.*, 2008], during a drought event linked to a warming of sea surface temperature in the tropical North Atlantic [*Marengo et al.*, 2008].

4.2. Threat of a Climatic Constraint Retreat for the Eastern Amazonia

[32] The IPCC models projecting significant climate change over the Amazon basin tend to reduce rainfall in eastern regions [*IPCC*, 2007; *Malhi et al.*, 2008], namely in the Brazilian states of Parà, Mato Grosso, Rondônia and eastern Amazonas. The gradient of anFDP in these regions is very gradual, such that small changes in precipitation result in a large increase in forest areas above HiFDP. In the upper quartile B1 run, 63% of the forest was susceptible to fire-driven deforestation, compared to 42% under current climate conditions. These regions also contain the most suitable soils for mechanized agriculture [*Jasinski et al.*, 2005; *Nepstad et al.*, 2008], and are likely to be under strong deforestation pressure in the coming decades [*Soares-Filho et al.*, 2006].

[33] Simulated reductions in dry-season precipitation suggest moderate reductions in precipitation during this period could render large areas of eastern Amazonia suitable for high or unlimited deforestation fire use. Further, these expansions happen twice as fast in the case of a seasonal change compared to a uniform change. This indicates that the occasional rain during the dry-season strongly limits ignitions over the considered 10-day period via STppt, and has an impact on following 10-day periods via LTppt. If these dry-season rainfall events disappear, fuel curing proceeds uninterrupted and fire prone conditions are reached earlier, potentially increasing the efficiency and number of repeated burns over a single dry-season. The seasonal precipitation change scenarios are consistent with rain-free periods during El Niño and other droughts.

4.3. Implications for Forest Conservation in Amazonia

[34] Deforestation and fires are expected to dominate forest changes relative to direct climate impact [*Barlow and Peres*, 2008; *Golding and Betts*, 2008]. Because fire is indispensable for large-scale forest conversion, the fate of the Amazon will greatly depend on the evolution of fire susceptibility and agricultural expansion.

[35] The fire threat stems from deforestation practices as studied here, as well as from understory fires. Understory fires induce significant tree mortality, and consecutive fire

events may reinitiate forest succession in which pioneer species replace primary forest trees, similar to secondary forests [*Barlow and Peres*, 2008]. Understory fires are more common in years of longer or stronger dry-seasons, and in areas of degraded or fragmented forest with high fuel loads and increased evapo-transpiration rates [*Alencar et al.*, 2006; *Elvidge et al.*, 2001]. Usually, they result from escaped fires (leakage fires) associated with deforestation and susbsequent agricultural activities. As such, droughts synchronize two essential factors for escaped fires (frequent ignitions and a dry understory), such that our anFDP metric may provide insights on the co-evolution of both deforestation feasibility and understory fire risk.

[36] Changes in deforestation potential also suggest probable changes in agricultural potential. Cultivated species are chosen to maximize yields within a certain range around optimal climatic and soil conditions [*Nepstad et al.*, 2008], spatially referred to as agricultural zoning. An increase in dry season severity, as described in this study, could alter agricultural potential in concert with changes in FDP, most likely shifting these zonings toward the remaining forest. Indeed, areas currently too wet for a given cultivar could turn suitable for cultivation in the case of longer dry seasons. Meanwhile, areas on the drier margins of the current zoning would turn too dry unless new adapted cultivars are developed, and the resulting loss in production would further increase the pressure for expansion on new lands. A study from the Brazilian Agricultural Research Corporation (EMBRAPA) and University of Campinas (UNICAMP) suggests that projected changes in temperature would decrease the suitable area for cultivation of most crop types in the Amazon [*Assad et al.*, 2008]. The spatial intersection of the HiFDP boundary with agricultural zoning may therefore be a major factor toward the expansion of agriculture in forested areas, or its intensification on degraded pastures with the generalization of crop rotation to maintain land fertility.

[37] Several limitations of the data and approach used in this study could be addressed with additional research. The FDP model was parameterized with 4 years of fire and precipitation data that do not represent the full range of climate variability in the Amazon region, especially because this period did not include strong El Niño and La Niña event (Figure 5). Precipitation is the only climate variable considered in our model of fire-driven deforestation, while a more detailed parameterization could also include other fire-relevant variables such as vegetation characteristics (e.g., fuel size) and temperature (see section 2.2). We acknowledge that although temperature is a secondary drought determinant in the Amazon (section 2.2), a significant warming trend would have the potential to affect FDP. Additionally, alterations of the hydrological cycle at the deforestation margins, referred to as edge effects, may accelerate fuel and soil moisture dynamics [*Pongratz et al.*, 2006; *Gash and Nobre*, 1997; *Camargo and Kapos*, 1995], which could lower the climatic barrier to burn in adjacent forests. Finally, the generalization of the model to other tropical forests frontiers of Africa and South East Asia would entail additional analyses to assess whether changes in deforestation practices, climatic conditions, and vegetation structure alter the climatic thresholds defined for the Amazon basin. Despite these potential differences, our approach based on climatic conditions is independent of other factors; the conceptual approach to define spatial constraints on fire-driven deforestation in this study should therefore apply to any land management and socio-economical context.

5. Conclusions

[38] In this study, we evaluated the climatic constraints on fire-driven deforestation in Amazonia using satellite-based fire detections and precipitation data. The model captures substantial intra and inter-annual deforestation dynamics, especially in low to intermediate fire potential regions where the climate-fire-deforestation link is strongest. Under average contemporary precipitation regimes, 1/3–1/2 of the projected advance of the deforestation frontier by 2050 would be limited by wet conditions in interior Amazon regions. However, climate change under the B1 emissions scenario may increase the potential for fire-driven deforestation across a wide range of Amazon forest types, although climate projections differ substantially between models. A simulation of seasonal changes indicated that a moderate reduction in precipitation (200 mm) during dry-season months could facilitate fire-driven deforestation in 76% of remaining forest areas.

[39] We thus suggest that the climatic influence on fire susceptibility is essential to consider for projections of future forest loss and agricultural expansion in Amazonia. Current deforestation models generally focus on socio-economic and drought stress direct impacts [*Ashton et al.*, 2008; *Soares-Filho et al.*, 2006]. Our findings provide complementary information to these projections, and most importantly should support the extension of these models to include the interaction between deforestation, fire, and climate.

References

Achard, F., R. DeFries, H. Eva, M. Hansen, P. Mayaux, and H. J. Stibig (2007), Pan-tropical monitoring of deforestation, *Environ. Res. Lett.*, *2*(4), 11.

Alencar, A., D. Nepstad, and M. D. V. Diaz (2006), Forest understory fire in the Brazilian Amazon in ENSO and non-ENSO years: Area burned and committed carbon emissions, *Earth Interact.*, *10*, 17.

Aragao, L., Y. Malhi, N. Barbier, A. Lima, Y. Shimabukuro, L. Anderson, and S. Saatchi (2008), Interactions between rainfall, deforestation and fires during recent years in the Brazilian Amazonia, *Philos. Trans. R. Soc. B*, *363*(1498), 1779–1785.

Arora, V. K., and G. J. Boer (2005), Fire as an interactive component of dynamic vegetation models, *J. Geophys. Res.*, *110*, G02008, doi:10.1029/2005JG000042.

Ashton, R., et al. (2008), How to include terrestrial carbon in developing nations in the overall climate change solution, Terrestrial Carbon Group.

Assad, E. D., et al. (2008), *Aquecimento Global e a Nova Geografia da produção Agrícola no Brasil*, 84 pp., Embaixada Britânica, Brasília.

Balmford, A., R. E. Green, and J. P. W. Scharlemann (2005), Sparing land for nature: Exploring the potential impact of changes in agricultural yield on the area needed for crop production, *Global Change Biol.*, *11*(10), 1594–1605.

Barlow, J., and C. A. Peres (2008), Fire-mediated dieback and compositional cascade in an Amazonian forest, *Philos. Trans. R. Soc. B*, *363*(1498), 1787–1794.

Broadbent, E. N., G. P. Asner, M. Keller, D. E. Knapp, P. J. C. Oliveira, and J. N. Silva (2008), Forest fragmentation and edge effects from deforestation and selective logging in the Brazilian Amazon, *Biol. Conserv.*, *141*(7), 1745–1757.

Camargo, J. L. C., and V. Kapos (1995), Complex edge effects on soil-moisture and microclimate in central Amazonian forest, *J. Trop. Ecol.*, *11*, 205–221.

Cardoso, M. F., G. C. Hurtt, B. Moore, C. A. Nobre, and E. M. Prins (2003), Projecting future fire activity in Amazonia, *Global Change Biol.*, *9*(5), 656–669.

Cardoso, M. F., C. A. Nobre, D. M. Lapola, M. D. Oyama, and G. Sampaio (2008), Long-term potential for fires in estimates of the occurrence of savannas in the tropics, *Global Ecol. Biogeogr.*, *17*(2), 222–235.

Carvalho, J. A., F. S. Costa, C. A. G. Veras, D. V. Sandberg, E. C. Alvarado, R. Gielow, A. M. Serra, and J. C. Santos (2001), Biomass fire consumption and carbon release rates of rainforest-clearing experiments conducted in northern Mato Grosso, Brazil, *J. Geophys. Res.*, *106*(D16), 17,877–17,887.

Cochrane, M. A., and W. F. Laurance (2008), Synergisms among fire, land use, and climate change in the Amazon, *Ambio*, *37*(7–8), 522–527.

Ebeling, J., and M. Yasue (2008), Generating carbon finance through avoided deforestation and its potential to create climatic, conservation and human development benefits, *Philos. Trans. R. Soc. B*, *363*(1498), 1917–1924.

Elvidge, C. D., V. R. Hobson, K. E. Baugh, J. B. Dietz, Y. E. Shimabukuro, T. Krug, E. M. L. M. Novo, and F. R. Echavarria (2001), DMSP-OLS estimation of tropical forest area impacted by surface fires in Roraima, Brazil: 1995 versus 1998, *Int. J. Remote Sens.*, *22*, 2661–2673.

Field, R. D., and S. S. P. Shen (2008), Predictability of carbon emissions from biomass burning in Indonesia from 1997 to 2006, *J. Geophys. Res.*, *113*, G04024, doi:10.1029/2008JG000694.

Gash, J. H. C., and C. A. Nobre (1997), Climatic effects of Amazonian deforestation: Some results from ABRACOS, *Bull. Am. Meteorol. Soc.*, *78*(5), 823–830.

Golding, N., and R. Betts (2008), Fire risk in Amazonia due to climate change in the HadCM3 climate model: Potential interactions with deforestation, *Global Biogeochem. Cycles*, *22*, GB4007, doi:10.1029/2007GB003166.

Hall, A. (2008), Better RED than dead: Paying the people for environmental services in Amazonia, *Philos. Trans. R. Soc. B*, *363*(1498), 1925–1932.

Hansen, M. C., Y. E. Shimabukuro, P. Potapov, and K. Pittman (2008), Comparing annual MODIS and PRODES forest cover change data for advancing monitoring of Brazilian forest cover, *Remote Sens. Environ.*, *112*(10), 3784–3793.

Holdsworth, A. R., and C. Uhl (1997), Fire in Amazonian selectively logged rain forest and the potential for fire reduction, *Ecol. Appl.*, *7*(2), 713–725.

Huffman, G. J., R. F. Adler, M. M. Morrissey, D. T. Bolvin, S. Curtis, R. Joyce, B. McGavock, and J. Susskind (2001), Global precipitation at one-degree daily resolution from multisatellite observations, *J. Hydrometeorol.*, *2*(1), 36–50.

Huffman, G. J., R. F. Adler, D. T. Bolvin, G. J. Gu, E. J. Nelkin, K. P. Bowman, Y. Hong, E. F. Stocker, and D. B. Wolff (2007), The TRMM multisatellite precipitation analysis (TMPA): Quasi-global, multiyear, combined-sensor precipitation estimates at fine scales, *J. Hydrometeorol.*, *8*(1), 38–55.

Intergovernmental Panel on Climate Change (IPCC) (2007), Climate change 2007: The physical science basis, in *Contribution of Working Group I to the Fourth Assessment Report of the Intergovernmental Panel on Climate Change*, edited by S. Solomon et al., Cambridge Univ. Press, New York.

Jasinski, E., D. Morton, R. DeFries, Y. Shimabukuro, L. Anderson, and M. Hansen (2005), Physical landscape correlates of the expansion of mechanized agriculture in Mato Grosso, Brazil, *Earth Interact.*, *9*, 18.

Justice, C. O., L. Giglio, S. Korontzi, J. Owens, J. T. Morisette, D. Roy, J. Descloitres, S. Alleaume, F. Petitcolin, and Y. Kaufman (2002), The MODIS fire products, *Remote Sens. Environ.*, *83*(1–2), 244–262.

Laurance, W. F., and G. B. Williamson (2001), Positive feedbacks among forest fragmentation, drought, and climate change in the Amazon, *Conserv. Biol.*, *15*(6), 1529–1535.

Malhi, Y., J. T. Roberts, R. A. Betts, T. J. Killeen, W. H. Li, and C. A. Nobre (2008), Climate change, deforestation, and the fate of the Amazon, *Science*, *319*(5860), 169–172.

Marengo, J. A., C. A. Nobre, J. Tomasella, M. D. Oyama, G. S. De Oliveira, R. De Oliveira, H. Camargo, L. M. Alves, and I. F. Brown (2008), The drought of Amazonia in 2005, *J. Clim.*, *21*(3), 495–516.

Mayle, F. E., and M. J. Power (2008), Impact of a drier Early Mid-Holocene climate upon Amazonian forests, *Philos. Trans. R. Soc. B*, *363*(1498), 1829–1838.

Mayle, F. E., R. P. Langstroth, R. A. Fisher, and P. Meir (2007), Long-term forest-savannah dynamics in the Bolivian Amazon: Implications for conservation, *Philos. Trans. R. Soc. B*, *362*(1478), 291–307.

Michalski, F., C. A. Peres, and I. R. Lake (2008), Deforestation dynamics in a fragmented region of southern Amazonia: Evaluation and future scenarios, *Environ. Conserv.*, *35*(2), 93–103.

Mitchell, T. D., and P. D. Jones (2005), An improved method of constructing a database of monthly climate observations and associated high-resolution grids, *Int. J. Climatol.*, *25*(6), 693–712.

Morton, D. C., R. S. DeFries, Y. E. Shimabukuro, L. O. Anderson, E. Arai, F. D. Espirito-Santo, R. Freitas, and J. Morisette (2006), Cropland expansion changes deforestation dynamics in the southern Brazilian Amazon, *Proc. Natl. Acad. Sci. U. S. A.*, *103*(39), 14,637–14,641.

Morton, D. C., R. S. Defries, J. T. Randerson, L. Giglio, W. Schroeder, and G. R. van Der Werf (2008), Agricultural intensification increases deforestation fire activity in Amazonia, *Global Change Biol.*, *14*(10), 2262–2275.

Naylor, R., H. Steinfeid, W. Falcon, J. Galloways, V. Smil, E. Bradford, J. Alder, and H. Mooney (2005), Losing the links between livestock and land, *Science*, *310*(5754), 1621–1622.

Nepstad, D., G. Carvalho, A. Cristina Barros, A. Alencar, J. Paulo Capobianco, J. Bishop, P. Moutinho, P. Lefebvre, U. Lopes Silva, and E. Prins (2001), Road paving, fire regime feedbacks, and the future of Amazon forests, *For. Ecol. Manage.*, *154*(3), 395–407.

Nepstad, D., P. Lefebvre, U. Lopes da Silva, J. Tomasella, P. Schlesinger, L. Solorzano, P. Moutinho, D. Ray, and J. Guerreira Benito (2004), Amazon drought and its implications for forest flammability and tree growth: A basin-wide analysis, *Global Change Biol.*, *10*(5), 704–717.

Nepstad, D., et al. (2006), Inhibition of Amazon deforestation and fire by parks and indigenous lands, *Conserv. Biol.*, *20*(1), 65–73.

Nepstad, D. C., C. M. Stickler, B. Soares, and F. Merry (2008), Interactions among Amazon land use, forests and climate: Prospects for a near-term forest tipping point, *Philos. Trans. R. Soc. B*, *363*(1498), 1737–1746.

Pongratz, J., L. Bounoua, R. S. DeFries, D. C. Morton, L. O. Anderson, W. Mauser, and C. A. Klink (2006), The impact of land cover change on surface energy and water balance in Mato Grosso, Brazil, *Earth Interact.*, *10*, 17.

Ray, D., D. Nepstad, and P. Moutinho (2005), Micrometeorological and canopy controls of fire susceptibility in a forested Amazon landscape, *Ecol. Appl.*, *15*(5), 1664–1678.

Saatchi, S. S., R. A. Houghton, R. Alvala, J. V. Soares, and Y. Yu (2007), Distribution of aboveground live biomass in the Amazon basin, *Global Change Biol.*, *13*(4), 816–837.

Schroeder, W., J. T. Morisette, I. Csiszar, L. Giglio, D. Morton, and C. O. Justice (2005), Characterizing vegetation fire dynamics in Brazil through multisatellite data: Common trends and practical issues, *Earth Interact.*, *9*, 1–26.

Schroeder, W., E. Prins, L. Giglio, I. Csiszar, C. Schmidt, J. Morisette, and D. Morton (2008), Validation of GOES and MODIS active fire detection products using ASTER and ETM+ data, *Remote Sens. Environ.*, *112*(5), 2711–2726.

Soares-Filho, B. S., D. C. Nepstad, L. M. Curran, G. C. Cerqueira, R. A. Garcia, C. A. Ramos, E. Voll, A. McDonald, P. Lefebvre, and P. Schlesinger (2006), Modelling conservation in the Amazon basin, *Nature*, *440*, 520–523.

Thonicke, K., S. Venevsky, S. Sitch, and W. Cramer (2001), The role of fire disturbance for global vegetation dynamics: Coupling fire into a Dynamic Global Vegetation Model, *Global Ecol. Biogeogr.*, *10*(6), 661–677.

Uhl, C., and J. B. Kauffman (1990), Deforestation, fire susceptibility, and potential responses to fire in the eastern Amazon, *Ecology*, *71*(2), 437–449.

van der Werf, G. R., D. C. Morton, R. S. DeFries, L. Giglio, J. T. Randerson, G. J. Collatz, and P. S. Kasibhatla (2008a), Estimates of fire emissions from an active deforestation region in the southern Amazon based on satellite data and biogeochemical modelling, *Biogeosciences Discuss.*, *5*(4), 3533–3573.

van der Werf, G. R., J. T. Randerson, L. Giglio, N. Gobron, and A. J. Dolman (2008b), Climate controls on the variability of fires in the tropics and subtropics, *Global Biogeochem. Cycles*, *22*, GB3028, doi:10.1029/2007GB003122.

Xie, P. P., and P. A. Arkin (1997), Global precipitation: A 17-year monthly analysis based on gauge observations, satellite estimates, and numerical model outputs, *Bull. Am. Meteorol. Soc.*, *78*(11), 2539–2558.

Y. Le Page and J. M. C. Pereira, Departamento de Engenharia Florestal, Instituto Superior de Agronomia, P-1349-017 Lisbon, Portugal. (niquya@gmail.com)

D. C. Morton, NASA Goddard Space Flight Center, Code 614.4, Greenbelt, MD 20771, USA.

G. R. van der Werf, Department of Hydrology and Geo-environmental Sciences, Faculty of Earth and Life Sciences, VU University Amsterdam, NL-1081 HV Amsterdam, Netherlands.